Optimized traffic flow at a single intersection: traffic responsive signalization

2004 J. Phys. A: Math. Gen. 37 561

(http://iopscience.iop.org/0305-4470/37/3/002)

INSTITUTE OF PHYSICS PUBLISHING JOURNAL OF PHYSICS A: MATHEMATICAL AND GENERAL

J. Phys. A: Math. Gen. **37** (2004) 561–576 PII: S0305-4470(04)64391-5

Optimized traffic flow at a single intersection: traffic responsive signalization

M Ebrahim Fouladvand, Zeinab Sadjadi and M Reza Shaebani

Department of Physics, Zanjan University, PO Box 313, Zanjan, Iran

Received 4 June 2003, in final form 17 October 2003
Published 7 January 2004
Online at stacks.iop.org/JPhysA/37/561 (DOI: 10.1088/0305-4470/37/3/002)

Abstract

We propose a stochastic model for the intersection of two urban streets. The vehicular traffic at the intersection is controlled by a set of traffic lights which can be operated subject to fix-time as well as traffic adaptive schemes. Vehicular dynamics is simulated within the framework of the probabilistic cellular automata and the delay experienced by the traffic at each individual street is evaluated for specified time intervals. Minimizing the total delay of both streets gives rise to the optimum signalization of traffic lights. We propose some traffic responsive signalization algorithms which are based on the concept of cut-off queue length and cut-off density.

PACS numbers: 45.70.Vn, 05.90.+m, 05.10.−a

This paper is dedicated to Professor Khajepour, co-founder of the Institute of Basic Studies in Advanced Sciences (IASBS), on the occasion of his 60th birthday.

1. Introduction

Modelled as a system of interacting particles driven far from equilibrium, *vehicular traffic* provides the possibility of studying various aspects of truly non-equilibrium systems which are of current interest in statistical physics [1–6]. For almost half a century, physicists have been challenged to understand the fundamental principles governing vehicular flow [4–7]. Recently, discrete models such as *cellular automata* have provided a significant theoretical framework for the discipline of traffic flow modelling. The first cellular automata, the so-called BML model, were introduced by *Biham, Middleton* and *Levine*. This model described a simplified network of urban intersections [8]. Soon after, cellular automata found their way into highway traffic through the pioneering work of *Nagel* and *Schreckenberg* [9] which became the ancestor of many papers in the literature (for a review see [1, 2] and the references therein). The BML model itself was later generalized to take into account several realistic features such as faulty traffic lights, independent turning of vehicles and green-wave synchronization [10–17]. The Nagel–Schreckenberg and BML model were recently combined to create an

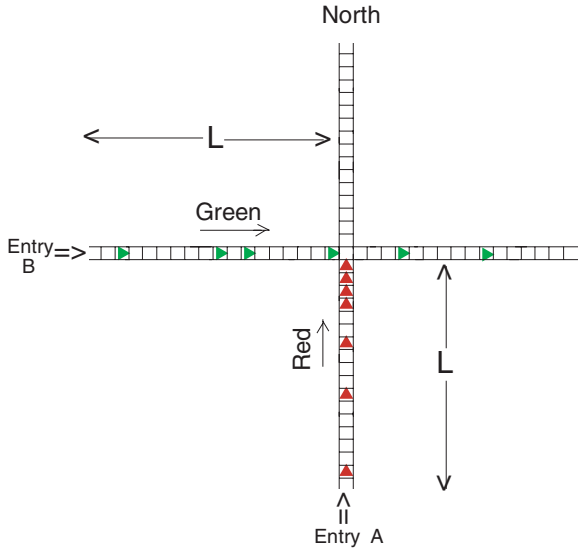

Figure 1. A schematic traffic flow at a one-way to one-way intersection.

upgraded version of city traffic models [18]. In a very recent paper, the model is now extended to account for different types of global signalization [19].

Despite the aforesaid efforts and those carried out by traffic engineers, the subject of optimal signalization of realistic urban networks has not yet been comprehensively reviewed. In the above approaches, the main concern has been focused on the global strategies of the traffic network and frequently the role of isolated intersections has been suppressed. We believe that the optimization of traffic flow at a single intersection is a substantial ingredient towards a global optimization. Isolated intersections are fundamental operating units of the sophisticated and correlated urban network and thorough analysis of them would be advantageous towards the ultimate task of the global optimization of the city network. In this regard, our objective in this paper is to analyse the traffic state of an isolated intersection in order to find a better insight into the problem. In addition to the theoretical viewpoint, an investigation of isolated intersections could be of practical importance. To a very good approximation, marginal intersections in cities are unaffected by other intersections and can be regarded as isolated. Generally there are two basic types of control for traffic lights at intersections: *fixed-cycle* and *traffic-responsive* [20, 21]. Both of these methods can be implemented via centralized or decentralized strategies. The application of each method strongly depends on traffic condition and the topology of the city network. In this paper, we study the basic features of traffic flow at a single intersection which is controlled both under fixed-cycle as well as traffic responsive schemes.

2. Formulation of the model

An isolated intersection is formed at the intersection of two streets. The streets, in principle, can each carry two opposite flows of vehicles. Depending on the design of the intersection, different phases of movement can be defined (a phase of traffic is defined as the flow of vehicles that proceed an intersection without conflict). Here for simplicity we restrict ourselves to the simplest structure: a *one-way to one-way* intersection (see figure 1). With no loss of

generality, we take the direction of the flow in the first street, hereafter referred to as street A, northwards. The other street (hereafter referred to as street B) conducts a one-way eastward flow. Cars arrive at the south and west entrances of the intersection. Space and time are discretized in such a way that each chain is divided into cells which are the same size as a typical car length. Time is assumed to elapse in discrete steps. We take the number of cells to be L for both roads. Each cell can be either occupied by a car or be empty. Moreover, each car can take discrete-valued velocities $1, 2, \ldots, v_{\max}$. To be more specific, at each step of time, the system is characterized by the position and velocity configurations of cars and the traffic light state at each road.

The system evolves under a generalized discrete-time Nagel–Schreckenberg (NS) dynamics. The generalized model incorporates anticipation effects of driving habits [22]. It modifies the standard NS model at its second step i.e., adjusting the velocities according to the space gap. Let us briefly explain the updating rules which are synchronously applied to all the vehicles. We denote the position, velocity and space gap (distance to the leading car) of a typical car at discrete time t by $x^{(t)}$, $v^{(t)}$ and $g^{(t)}$ and the same quantities for the leading car by $x_l^{(t)}$, $v_l^{(t)}$ and $g_l^{(t)}$. Assuming that the expected velocity of the leading car, anticipated by its follower, in the next time step $t+1$ takes the form $v_{l,\text{anti}}^{(t)} = \min\bigl(g_l^{(t)}, v_l^{(t)}\bigr)$, we define the effective gap as $g_{\text{eff}}^{(t)} := g^{(t)} + \max\bigl(v_{l,\text{anti}}^{(t)} - \text{gap}_{\text{secure}}, 0\bigr)$ in which $\text{gap}_{\text{secure}}$ is the minimal security gap. Concerning the above considerations, the following updating steps evolve the position and the velocity of each car:

(1) Acceleration:

$$v^{(t+1/3)} := \min(v^{(t)} + 1, v_{\max}).$$

(2) Velocity adjustment:

$$v^{(t+2/3)} := \min\bigl(g_{\text{eff}}^{(t+1/3)}, v^{(t+1/3)}\bigr).$$

(3) Random breaking with probability p: if random $< p$ then $v^{(t+1)} := \max(v^{(t+2/3)} - 1, 0)$.
(4) Movement: $x^{(t+1)} := x^{(t)} + v^{(t+1)}$.

Let us now specify the physical values of our time and space units. Ignoring the possibility of existence of long vehicles such as buses, trucks, etc, the length of each cell is taken to be 5.6 m which is the typical bumper-to-bumper distance of cars in a waiting queue. Concerning the fact that in most urban areas a speed-limit of 60 km h^{-1} should be kept by drivers, we quantify the time step in such a way that $v_{\max} = 6$ corresponds to the speed-limit value (taken as 60 km h^{-1}). In this regard, each time step equals 2 s and therefore each discrete increment of velocity signifies a value of 10 km h^{-1} which is equivalent to a comfortable acceleration of 1.4 m s^{-2}. We have also set the horizon length $L = 70$ cells and $\text{gap}_{\text{secure}} = 1$. The state of the system at time $t+1$ is updated from that at time t by applying the modified NS dynamical rules.

Step 1: signal determination. We first specify the signal states for all of the driving directions. In subsequent sections we will, in detail, explain the scheme with which the traffic lights change their colour.

Step 2: movement in the green road. At this stage, we update the position and velocities of cars on the green road according to the movement rules which are synchronously applied to each car.

Step 3: movement in the red road, delay evaluation. Here the updating is divided into two parts. In the first part, we evaluate the delay of cars waiting on the red period of the signalization. In the second half, we update the position and velocities of the moving cars approaching the waiting queue. We should note that once the signal switches to red, the moving cars continue their movement until they come to a complete stop when reaching the end of the waiting queue. As soon as a car comes to halt, it contributes to the total delay. In order to evaluate the delay, we measure the queue length (the number of stopped cars) at time step t and denote it by the variable Q. We recall that $\mathrm{pos}^{\mathrm{red}}[i, t] = 1$ for $i = 1, \ldots, Q$ and zero at $i = Q + 1$. Delay at time step $t + 1$ is obtained by adding the queue length Q to the delay at time step t.

$$\mathrm{delay}(t + 1) = \mathrm{delay}(t) + Q(t). \tag{1}$$

This ensures that during the next time step, all the stopped cars contribute one step of time to the delay. The next part describes the update of positions and velocities of moving cars. Moving cars can potentially be found in the cells $Q + 2, Q + 3, \ldots, L$. We update their positions and velocities accordingly.

Step 4: entrance of cars to the intersection. So far, we have dealt with those cars within the horizon of the intersection which goes up to the entry point located at site L. Here we discuss the entrance of cars into the intersection. Generally speaking, during each green period, a fraction of the queue will dissolve and pass the intersection. If the average arrival rate of cars exceeds the maximum evacuation rate of the lane, then, on average, a fraction of a generic queue will not be able to go through the intersection and should wait until the next green period arrives. Correspondingly in the course of time, the remainders accumulate giving rise to a growing queue length. In reality we rarely observe these phenomena since an actual intersection is linked to others, hence the possibility of such a rare event is restricted to very exceptional cases where there is an overwhelming large amount of incoming flux. Throughout the paper, we assume that the average in-flow rate is sufficiently below this evacuation rate so that a generic queue will have enough green time to dissolve and that the intersection is able to support the incoming flux. In this case, there is a typical queue length which affects the motion of incoming cars. The motion of a car approaching the red light is affected via two factors: the distance to the end of the queue and the traffic light signal which act as a hindrance to the incoming traffic flow. In the light traffic state under consideration, there exists an interaction distance to the queue beyond which one can, to a good extent, assume that the cars are moving without being affected by the traffic light signal. Away from this interaction zone, the cars move according to the movement rules without any hindrance. We take the position of the place at which the cars enter the horizon of the intersection to be 70 cells, equivalent to 400 m. The time head-ways between cars entering at this location vary in a random manner which consequently implies a random distance headway between successive entering cars. As a candidate for describing the statistical behaviour of the random space gap of entering cars, we have chosen a Poisson distribution. The Poisson distribution function has been used in a variety of phenomena incorporating the modelling of 'queue theories' and has proved to be a good estimation of reality [23]. In addition, it has the merit of taking only discrete values which is desirable to us in the view of the fact that in our model the gap is a discrete variable. According to this distribution function the probability that the space gap between the car entering the intersection horizon and its predecessor is n is: $p(n) = \frac{\lambda^n \mathrm{e}^{-\lambda}}{n!}$ where the parameter λ specifies the average as well as the variance of the distribution function. The parameter λ is a direct measurement of traffic volume. A large value of λ describes light traffic while on the other hand, a small value of λ corresponds to heavy traffic. Now we let the cars enter the intersection's horizon. At the end of the movement

rule, we evaluate the position of the farthest cars on both streets. We denote them by last_A and last_B. By definition, $\text{pos}_\text{A}[j, t] = 0$ for $j > \text{last}_\text{A}$. A similar statement applies to street B. In order to simulate the entrance of cars into the horizon of the intersection, we randomly choose an integer weighted by the Poisson distribution function. This number represents the gap of the oncoming successor of the farthest car. Let us denote these numbers (headways) by h_A and h_B for streets A and B, respectively. Once the random gap is chosen, we create a car at the position $\text{last}_\text{A} + h_\text{A}$ ($\text{last}_\text{B} + h_\text{B}$) of the street A (B), respectively. The created car survives provided the following constraint is satisfied: $\text{last}_\text{A} + h_\text{A} \leqslant L$ ($\text{last}_\text{B} + h_\text{B} \leqslant L$). If the position of the created car exceeds the horizon length L, the creation procedure is rejected. The above *ad hoc* rules update the configuration of the intersection in time. In the following section, we will explain our simulation results.

3. Signalization of traffic lights: fixed time scheme

In this controlling scheme, the traffic flow is controlled by a set of traffic lights which are operated in a fixed-cycle manner. The lights periodically go green with a fixed period (cycle length) T. This period is divided into two parts: in the first part, the traffic light is green for street A (simultaneously red for street B). This part lasts for T_g s ($T_g < T$). In the second part, the lights change colour and movement is allowed for the cars of road B. The second part lasts from T_g to T. This behaviour is repeated periodically. Cars enter the intersection and a fraction of them experience the red light and consequently have to wait until they are allowed to go through the intersection during the upcoming green periods. Now we raise the basic question: how should one adjust the ratio of $\frac{T_\text{green}}{T}$ in order to optimize the throughput flow?.

There is now an almost well-established agreement on the quantitative definition of optimization. Borrowing from the traffic engineering literature, we adopt *optimized traffic* as a state in which the total delay of vehicles is minimum. In one of our preceding works [24], we analytically evaluated the total delay in terms of arrival as well as that of the exit rates of vehicles. However, our approach was based on the simple assumption of time-constancy of the arrival rates. In reality, we know that successive cars arrive with fluctuating time-headways which consequently induces time-varying arrival rates. In this paper, we address the question of non-constant rates. In order to evaluate the delay, we have simulated the flow of vehicles. For the sake of simplicity, we have assumed that each street has a single lane. For streets with more than one lane, one should simply multiply the value of delay by the number of lanes.

3.1. Simulation results: symmetric inflow

We let the intersection evolve for 1800 time steps which is equal to a real time period of 1 h. We let the green time of street A, T_g, vary from zero to T. For each value of T_g, we evaluate the aggregate delay corresponding to both traffic lights during 1800 time steps. We have averaged the results of 50 independent runs of the program. Let us first consider the symmetric traffic states in which the traffic conditions are equal for both roads. In this case, we equally load the intersection with entering cars spatially separated by random space gaps (Poisson statistics) from each other. Figures 2 and 3 depict the total delay curves as a function of T_g allocated to road A for two values of cycle length.

The general shape of the total delay curve resembles a 'U-shaped' valley. The middle area, where the total waiting time is minimized, corresponds to a situation in which the evacuation rate of roads exceeds the in-flow and the queues can be dissolved during one green period and consequently all the waiting cars will be able go through the intersection in the upcoming green period. The optimal traffic flow is obtained by keeping the lights at equal timing $T_g = \frac{T}{2}$.

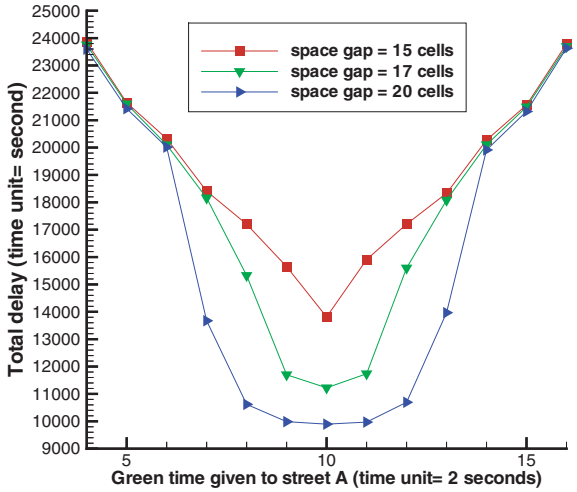

Figure 2. Total delay versus the green time of road A is sketched for various in-flow rates. The cycle length is 40 s in this graph.

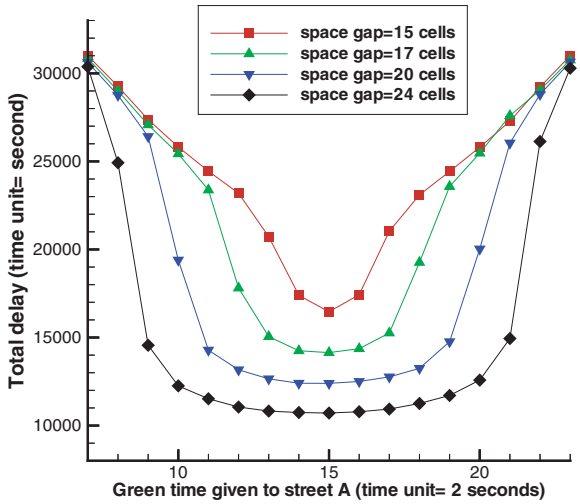

Figure 3. Total delay versus the green time of road A is sketched for various in-flow rates. The cycle length is 60 s in this graph.

Before preceding further, it would be useful to discuss, in detail, the conditions in which the intersection would not able to support the in-flux and hence the queue length starts growing. Supposing the fraction $\frac{T_g}{T}$ of the cycle is given as green time to a street say A. Therefore during the 1 h time interval, street A receives $3600\frac{T_g}{T}$ s of green time. Using the fact that in green phase vehicles are going through the crossing with the approximate rate of 0.5 s^{-1} per lane, on average, the maximum out-flow capacity, denoted by $\langle C_{\max}\rangle$ would be: $\langle C_{\max}\rangle = 1800\frac{T_g}{T}$. On the other hand, the total number of in-flow can be estimated once the average space gap is given. To do so, we first obtain the average time headway of entering vehicles (in second), denoted by Δ_{λ_A}, as follows: $\Delta_{\lambda_A} = 5.6\frac{\lambda_A}{v_{\max}}$. In the above formula, we have assumed that

entering cars have the maximum velocity and 5.6 denotes the cell length in metres. Concerning the above consideration, during 1 h, the average number of entering cars is approximated by $\langle N_{\text{in}} \rangle = \frac{3600}{\Delta_{\lambda_A}}$. Avoiding the occurrence of a growing queue leads to the satisfaction of the following constraint [24]:

$$\langle N_{\text{in}} \rangle \leqslant \langle C_{\text{max}} \rangle. \tag{2}$$

Substituting maximum velocity by 16.7 m s^{-1} in the above constraint, gives rise to condition $T_g \geqslant \frac{6T}{\lambda_A}$. Taking $T = 60$ s, the minimum consistent value of T_g for $\lambda = 13$, 16 and 19 cells would be 27, 22 and 19 s, respectively. Alternatively, the lowest λ_A is restricted to 12 cells or 67 m. Similar arguments should be applied to street B. Concerning the fact that the green time of street B is $T - T_g$, one simply deduces that the condition $T - T_g \geqslant \frac{6T}{\lambda_B}$ should hold. Combining the two conditions on T_g, one arrives at the following inequality on T_g for a stationary condition of the queues.

$$\frac{6T}{\lambda_A} \leqslant T_g \leqslant T\left(1 - \frac{6}{\lambda_B}\right). \tag{3}$$

Consequently, the allowed λ_A, λ_B and T_g should satisfy the above inequality, otherwise the queue will grow infinitely in time. From the above relation, one concludes two necessary conditions on the rates: $\lambda_B \geqslant 6$ and $\frac{1}{\lambda_A} + \frac{1}{\lambda_B} \leqslant \frac{1}{6}$ which hold regardless of the value of green time. We note that the above arguments are based on simple mean-field approximation and no fluctuation has been taken into account. There are two origins of fluctuation, the first one concerns the stochastic space gap of cars which make the incoming flux deviate from constant, and second, the interaction among cars and randomness arising from the car movements. Therefore the region close to critical volume $\lambda_A = 12$ needs special treatment. Simulation results show that away from the critical region, fluctuations do not violate our mean-field conclusions.

3.2. Asymmetric in-flow rates

In the asymmetric states, the entering rates into the roads differ from each other. An interesting asymmetric state is the intersection of a major to a minor street. A large fraction of urban intersections lies in the category of major-to-minor. The signalization of these types of crossing is still a controversial subject. The main reason is that in most intelligent real-time controller systems, the signalization of these intersections is highly affected by the major intersections signalization schemes which frequently overlook the local optimization of minor intersections. In our model, a major-to-minor crossing is modelled by light traffic in one road and congested traffic in the other road. Figure 4 depicts the behaviour of the delay curve at a major-to-minor intersection. As observed, the minima of delay curves are shifted towards the right which expresses the fact that the majority of green time should be given to the road with the higher in-flow rate. Analytical considerations lead to a distribution of green times in proportion to the in-flow rates of the roads [24]. To be more specific, let us denote the average arrival rates at streets A and B by α_A and α_B. Note that α_A and α_B are proportional to the inverse of entering space gaps. We now evaluate the waiting time of street A during one complete cycle. The number of cars arriving at the queue during the time interval $[t, t + \mathrm{d}t]$ in the red period, which lasts $T - T_g$ s, is $\alpha_A\,\mathrm{d}t$. These cars should wait $T - T_g - t$ s until the upcoming green period starts. Therefore, their contribution to delay reads $\alpha_A\,\mathrm{d}t\,(T - T_g - t)$. The aggregate delay of street A during the cycle is obtained by summation of infinitesimal delays as follows:

$$\int_0^{T-T_g} \alpha_A\,\mathrm{d}t\,(T - T_g - t) = \frac{1}{2}\alpha_A (T - T_g)^2. \tag{4}$$

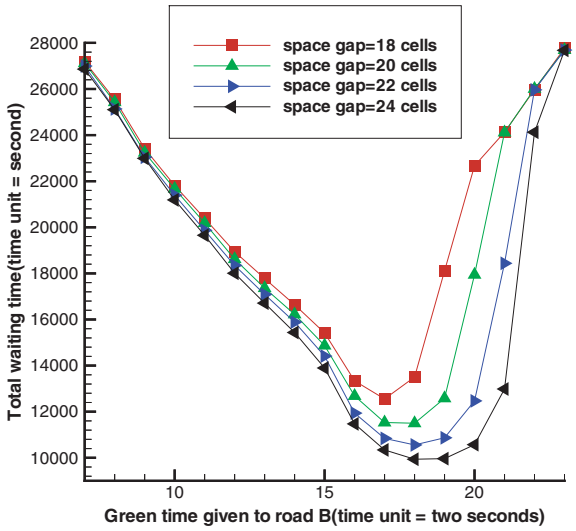

Figure 4. Total delay for asymmetric traffic volumes in a major-to-minor crossroads. The space gap of the major road is set to 13. The space gap of the minor road is varied. $T = 60$ s.

Similarly the contribution of street B to total delay can simply be evaluated as $\frac{1}{2}\alpha_{\mathrm{B}} T_g^2$. Adding the street delays together and minimizing with respect to T_g gives rise to the optimal T_g:

$$T_g^{\mathrm{opt}} = \frac{\alpha_{\mathrm{A}}}{\alpha_{\mathrm{A}} + \alpha_{\mathrm{B}}} T. \tag{5}$$

The above result corresponds to a distribution of green times in the ratio of in-flow rates. Our simulation results are in good agreement with this conclusion. In fact the positions of optimal green times, i.e., the minima of the delay curves, grow linearly with the linear decrease of in-flow rates which are in turn proportional to the inverse of the average space gap.

4. Signalization of traffic lights: traffic adaptive

We now discuss the traffic adaptive controlling scheme in which the light signalization is adapted to the traffic at the intersection. Nowadays advanced traffic control systems anticipate the traffic approaching intersections. Traffic-responsive methods have shown very good performance in controlling city traffic and now a variety of schemes exists in the literature [20, 21, 25, 26]. In these schemes, the data obtained via traffic detectors installed at the intersection are gathered for each movement direction and it is possible to count the queue lengths formed behind the red lights. One can also measure the time-headways between successive cars passing each lane detector. Thus it is possible to estimate the traffic volume existing at the intersection. There are various methods for distribution of green times. In what follows we try to explain some standard ones. In each scheme, the green time of a typical green street is terminated if some conditions are fulfilled. By green (red) street we mean the street for which the traffic light is green (red). We now state the termination conditions for each scheme.

Scheme (1). The queue length in the conflicting direction exceeds a cut-off value L_c. This scheme only concerns the traffic states in the red street.

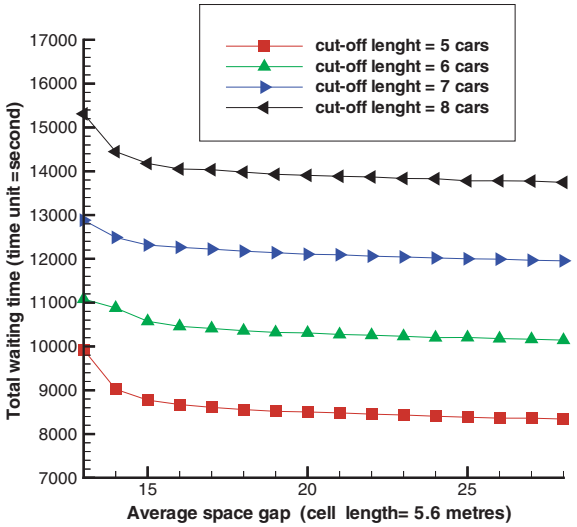

Figure 5. Total delay in terms of average space gap of entering cars for some cut-off queue length $L_c = 5, 6, 7, 8$.

Scheme (2). The global car density in the green street falls below the cut-off value ρ_c. Here the algorithm only considers the traffic state in the green street.

Scheme (3). Each direction is endowed with two control parameters L_c and ρ_c. The green phase is terminated if the conditions: $\rho^{\mathrm{g}} \leqslant \rho_c$ and $L^{\mathrm{r}} \geqslant L_c$ are both satisfied.

Here the algorithm implements the traffic states in both streets. The superscripts 'r' and 'g' refer to the words 'red' and 'green', respectively. We note that the first two schemes are special cases of the more general scheme (3). Schemes (1) and (2) are the limiting cases of schemes (3) by letting $\rho_c \to 1$ and $L_c \to 0$, respectively. In general, the numerical values of control parameters L_c and ρ_c could be taken different for each individual street. In what follows we present our simulation results for the different types of signalization schemes introduced above.

4.1. Simulation results: symmetric inflow

We let the intersection evolve for 1800 time steps which is equal to a real time period of 1 h. We evaluate the aggregate delay for both streets as well the number of passed vehicle during 1800 time steps in each direction for different traffic situations. For the first situation, we have considered the symmetric traffic state in which the traffic conditions are equal for two streets. In this case, we equally load the streets with entering cars spatially separated from each other by random space gaps, obeying Poisson statistics. We first discuss the first scheme in which the lights change colour as soon as the queue length reaches the cut-off length. We set an equal cut-off length for both streets. Figure 5 depicts the total delay curve as a function of traffic volume for various cut-off lengths.

We observe that for each cut-off length, the total delay shows a slight decrease with respect to the in-flow rate. Figure 5 demonstrates that the shorter the cut-off length, the less the total delay. Figure 6 shows the delay versus in-flow rate when the lights are signalized according to scheme (2). Here the green light is terminated below a certain occupancy in the corresponding moving flow.

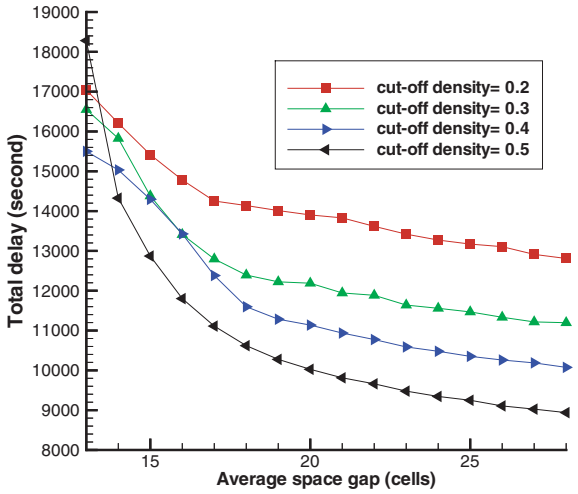

Figure 6. Total delay in terms of average space gap of entering cars for some cut-off densities.

We observe that the first scheme gives rise to less delay. The reason is that in relatively low traffic volume, more cars have to stop at the red light in order that the global density in the green direction reaches its cut-off value. This raises the delay compared to scheme (1). Finally we discuss the third scheme in which two conditions should be satisfied for termination of the green light. In this scheme, both cut-off densities and cut-off lengths are taking into account. We have investigated the case where cut-off parameters are equal for both streets i.e., $\rho_c^{\mathrm{A}} = \rho_c^{\mathrm{B}} = \rho_c$ and $L_c^{(\mathrm{A})} = L_c^{(\mathrm{B})} = L_c$. The following table shows the delay table of 1 h performance for various values of ρ_c and L_c. Traffic in-flow rates are $\lambda_{\mathrm{A}} = \lambda_{\mathrm{B}} = 13$.

	L_c				
ρ_c	5	6	7	8	9
0.10	14 000	15 500	15 900	17 900	18 600
0.20	13 200	14 900	14 700	16 500	17 400
0.30	11 500	12 800	13 200	15 500	16 400
0.40	11 200	11 900	12 600	14 000	15 300
0.50	10 900	11 200	11 700	12 700	13 900

The above result sets the optimal parameters at $\rho_c = 0.5$ and $L_c = 5$. We have tested a variety of other traffic volumes. The results demonstrate that in the control parameter space, the optimal region lies in high ρ_c and low L_c. The above result shows that scheme (3) gives an improved delay with respect to scheme (2). Our simulation results show that this conclusion can be made for other values of λ hence the third scheme is more optimal than the second one. However, the results show that the first scheme still gives lower delays compared with scheme (3). Specifically for $\lambda = 20$ cells, the predicted delays are 8500, 10100 and 9600 s, respectively. The next graphs depict the behaviour of the consecutive green times of streets. We have chosen the green times of street A. Fluctuating traffic volume in the streets induces fluctuating green periods which are known as the *green time plans* in the traffic engineering literature [21, 26]. We note that a realistic optimizing algorithm must satisfy the constraint that the duration of green phases should not be shorter that a minimal amount, e.g. 10 s or so. This minimal value reflects the actual time required for an immobile waiting queue to

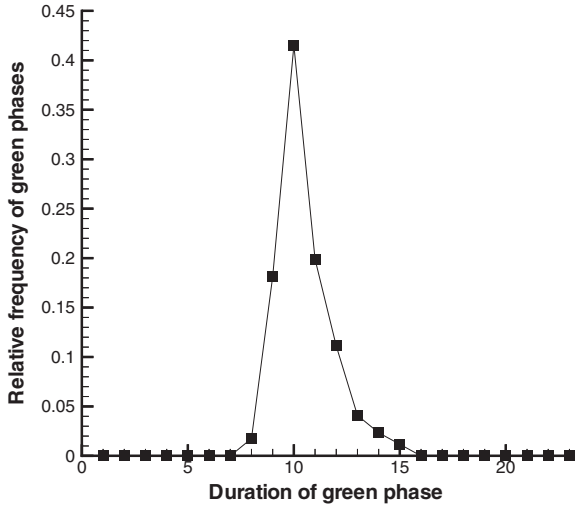

Figure 7. Green times histogram of street A. $\lambda_A = \lambda_B = 13$ cells. The lights are controlled via scheme (1). The cut-off length is taken as 7 cars.

accelerate and make a considerable movement forward. Our simulation results show that $L_c \geqslant 4$ corresponds to typical green periods greater than 12 s. It may be useful to analyse the statistics of green plans. Denoting the consecutive green times by $T_g^{(1)}, T_g^{(2)}, T_g^{(3)}, \ldots$, we first obtain the basic statistical properties which are the moments of the distribution of the green times. Figure 7 shows the green plan histogram of street A for $\lambda_A = \lambda_B = 13$. For the mentioned traffic state, the average green time and the standard deviation of street A are 18 and 2.54 s, respectively.

4.2. Asymmetric in-flow

Scheme (1). We now investigate the situations where the streets are not equally loaded. For this purpose, we fix the in-flow rate of street A at $\lambda_A = 13$ and vary the in-flow rate of street B. Figure 8 exhibits the total waiting time curves as well as those of each street for some cut-off lengths (taken equal for both streets). Here again less delay is achieved for shorter cut-off lengths which in turn correspond to shorter green phases.

We observe that decreasing the traffic volume in street B leads to a decrease in total delay as expected. In figure 9, the dependence of each street delay on the traffic volume of street B is exhibited in detail. One observes that the delay of street B starts growing whereas that of street A decreases. This shows that the algorithm does not always act optimally for individual directions. In fact, the delay of street A, which is more congested than street B, behaves decreasingly while the delay of the less congested street, B, behaves increasingly. Nevertheless, the algorithm acts in an optimal manner when taking into account the whole intersection.

We have also examined the cases where cut-off lengths take different values for streets with non-equal incoming flux. Simulation results show that optimal cut-off lengths should be taken equal and as short as possible. For instance, in the case $\lambda_A = 14$ and $\lambda_B = 24$ the minimized total delay is 8500 s when $L_c^{(A)} = L_c^{(B)} = 5$.

Scheme (2). Let us now investigate the predictions of scheme (2). As explained, in this method, once the global density of the moving direction (in the vicinity of the intersection)

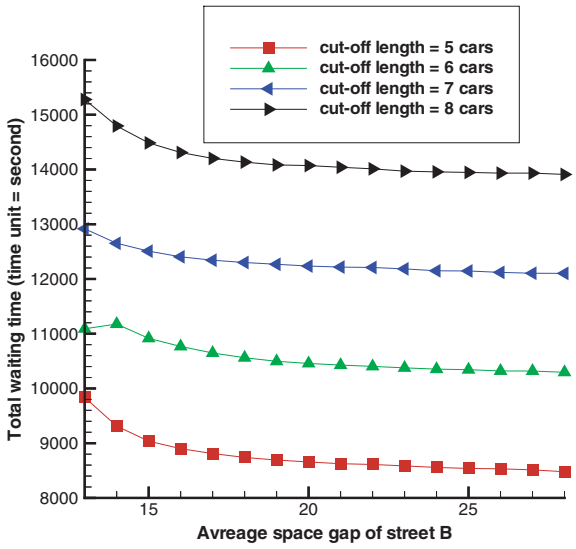

Figure 8. Total delay versus the inverse traffic volume of street B for various cut-off lengths. λ_A is fixed at 13.

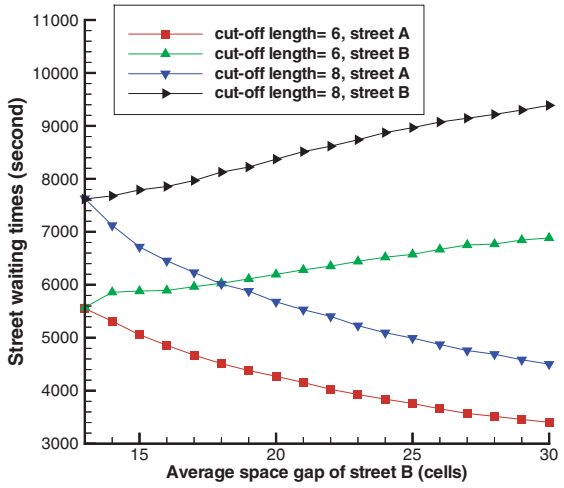

Figure 9. Delay of individual streets as a function of inverse traffic volume of street B. Traffic volume of street A is kept fixed at $\lambda_A = 13$.

falls below the cut-off density, the green phase is terminated irrespective of the queue length in the red direction. The global density is obtained by measuring the occupancy of L_ρ cells before the crossing point. The following graphs show the 1 h delay behaviour of individual streets as well as that of the entire intersection for various controlling densities (figure 10). Analogous to the predictions of the first scheme, here the algorithm increases the delay in the minor road whereas the delay is decreased in the major road upon decreasing the traffic volume in the minor road.

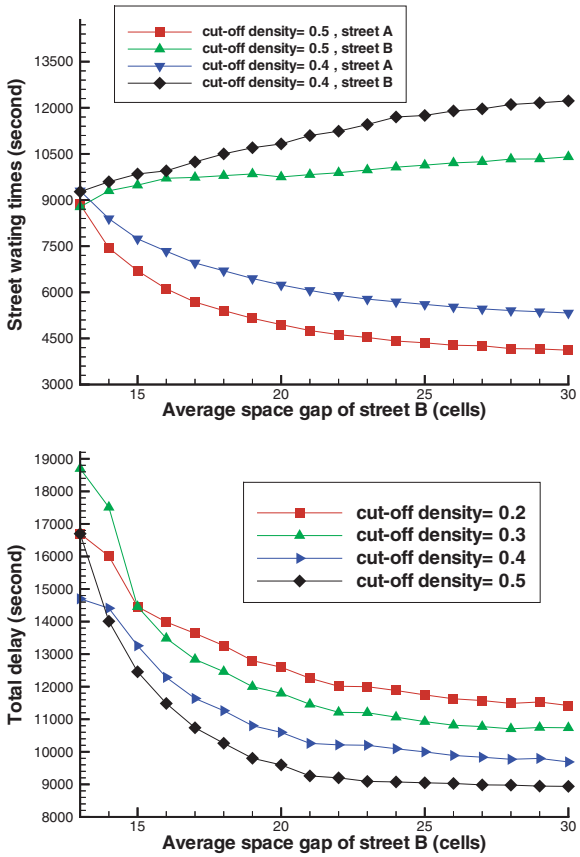

Figure 10. Top: delay of individual streets as a function of inverse traffic volume of the minor street B. Traffic volume of street A (major street) is kept fixed at $\lambda_A = 13$ cells. Bottom: total delay versus the inverse traffic volume in the minor street for various controlling densities.

One observes that the delay predictions of the second scheme are higher than those of the first scheme. We have also examined the cases where cut-off densities of each street take non-equal values. The following table exhibits the values of 1 h total delay for various amounts of cut-off densities of each street. Traffic volumes correspond to $\lambda_A = 13$ and $\lambda_B = 18$ and L_ρ is set to 10 cells.

	ρ_A				
ρ_B	0.10	0.20	0.30	0.40	0.50
0.10	14 800	17 100	21 000	20 900	21 100
0.20	13 700	15 400	15 600	16 700	16 500
0.30	12 900	13 300	13 700	14 400	14 600
0.40	11 400	12 100	13 200	14 200	14 000
0.50	10 800	11 300	11 800	12 400	12 900
0.60	10 600	10 800	10 700	10 900	11 000

We observe that optimal flow corresponds to setting $\rho_A = 0.1$ and $\rho_B = 0.6$. In contrast to scheme (1) where optimal cut-off lengths are equal to each other, here we see that in asymmetric traffic volume, the optimal cut-off densities are non-equal. We note that other values of cut-off densities give rise to unrealistic green time plans and hence are excluded from the table. It would be useful to compare the minimal delay with the predicted one in scheme (1). For the traffic volumes corresponding to $\lambda_A = 13$ and $\lambda_B = 18$, scheme (2) gives the minimal delay at 10 600 s whereas scheme (1) predicts the value 8700 s for $L_c = 5$. We have also obtained the total delay table for another asymmetric traffic volume where in-flow rates are $\lambda_A = 13$ and $\lambda_B = 25$. For this choice of traffic volumes, the optimal cut-off densities are $\rho_A = 0.10$ and $\rho_B = 0.40$ which are relatively close to the preceding optimal values. The values of minimal delays are 9300 and 8500 s in schemes (2) and (1), respectively. We have investigated a variety of traffic states corresponding to different in-flow rates. The results show that scheme (1) gives better optimal states than scheme (2). Before discussing scheme (3), we would like to discuss the role of parameter L_ρ. In fact, the measurement of global density depends on the length L_ρ. This length itself could be regarded as a control parameter. We have carried out simulations for various values of L_ρ. Our results show that $L_\rho = 10$ corresponds to the best choice. For instance the result obtained for the same traffic state investigated in the above table and $L_\rho = 12$ gives the optimal delay as 11 000 s which is higher than the value predicted by $L_\rho = 10$.

Scheme (3). Finally we discuss the third scheme. In this scheme both cut-off densities and cut-off lengths are taking into account. The following graphs show the 1 h delay behaviour of individual streets as well as that of the entire intersection for various controlling densities (figure 11). Analogous to the predictions of the first and second schemes, here the algorithm increases the delay in the minor road whereas the delay is decreased in the major road upon decreasing the traffic volume in the minor road. We have taken the cut-off parameters equal for both streets i.e., $L_c^A = L_c^B$ and $\rho_c^A = \rho_c^B$.

Another investigation considers the effect of cut-off densities for fixed values of cut-off lengths. The following table exhibits the delay when $\lambda_A = 13$ and $\lambda_B = 18$. $L_c = 5$ while ρ_c is varied.

	ρ_c^B				
ρ_c^A	0.10	0.20	0.30	0.40	0.50
0.10	12 560	11 600	11 300	11 000	10 800
0.20	12 400	11 370	10 950	10 600	10 500
0.30	12 250	11 200	10 560	10 300	9 960
0.40	12 160	11 150	10 470	10 200	9 980
0.50	11 950	10 780	10 350	9 970	9 900

The table above shows that optimal traffic flow is obtained in the high–high region of the (ρ_c^A, ρ_c^B) sub-space of control parameters. The minimized delay is 9900 s. For the same in-flow rates, the values of minimal delays predicted by schemes (2) and (1) are 10 600 and 8700 s, respectively. This comparison shows that the third scheme acts better than scheme (2) but is less efficient than the first scheme. Further simulation results carried out for other traffic states demonstrate that for $\lambda_B \leqslant 19$ (λ_A fixed) scheme (3) acts better than scheme (2) but is less efficient than scheme (2) for higher in-flow rate of the minor street. Nevertheless, scheme (1) gives the least delay for all asymmetric states.

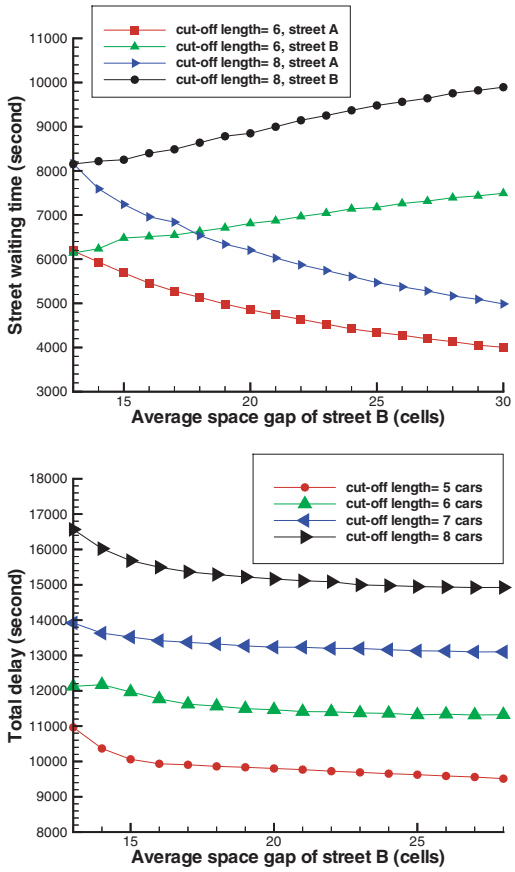

Figure 11. Top: delay of individual streets as a function of traffic volume of the minor street B. Traffic volume of street A (major street) is kept fixed at $\lambda_A = 13$ cells. Bottom: total delay versus the traffic volume in the minor street for various controlling densities. Cut-off densities are taken as 0.5 for both streets.

5. Summary and concluding remarks

In this paper, we have investigated the optimization of vehicular traffic flow at an isolated signalized intersection in the framework of cellular automata. Marginal urban areas are places where single intersections are frequently designed and operated. Investigations on single junctions can be of practical relevance for various applications in city traffic. Basically there are two methods of signalization of the traffic lights: fixed-time or adaptive. In traffic adaptive strategies, it has always been a subject of argument whether to control an intersection under a centralized or decentralized scheme. In special circumstances, decentralized local adaptive strategies operate more effectively than globally adaptive strategies [20, 21, 25–28] and often show very good performance. For this purpose, we have developed and analysed prescriptions for the traffic light signalization at single intersections. Our simulation results confirm that in a fixed-time scheme, green times should be distributed proportional to the traffic in-flow rates. We have simulated and analysed three traffic responsive signalization schemes. The signalization mechanisms are based on the concepts of cut-off queue lengths and densities. Two major conclusions can be drawn from our simulation results. First, the traffic adaptive

scheme acts more optimally than the fixed-time one. Secondly, the best traffic adaptive scheme is the one in which the flow in the green direction is terminated as soon as the queue length in the opposite direction exceeds the cut-off value L_c. In this method, the traffic states in the green direction are not taken into account. It should be noted that the results in this paper have been obtained under a modified version of the Nagel–Schreckenberg model. Whether these results are robust against more realistic vehicle movement models needs more exploration and is the subject of our current investigation. Throughout the paper we have used Poisson statistics for the headway of approaching cars. However, realistic in-flow traffic would certainly deviate from this statistics. Investigations on the impact of the entrance statistics on the above results will shed more light on the problem.

Acknowledgments

We would like to express our gratitude to Nima Hamedani Radja for his fruitful and enlightening discussions. Special thanks go to Richard Sorfleet for reading the manuscript.

References

[1] Chowdhury D, Santen L and Schadschneider A 2000 *Phys. Rep.* **329** 199
[2] Helbing D 2001 *Rev. Mod. Phys.* **73** 1067
Helbing D 1997 *Vehrkersdynamik: Neue Physikalische Modellierungskonzepte* (Berlin: Springer)
[3] Kerner B S 2001 *Networks Spatial Econ.* **1** 35
[4] Wolf D E, Schreckenberg M and Bachem A (ed) 1996 *Traffic and Granular Flow* (Singapore: World Scientific)
[5] Wolf D E and Schreckenberg M (ed) 1998 *Traffic and Granular Flow* (Singapore: Springer)
[6] Herrmann H J, Helbing D, Schreckenberg M and Wolf D E (ed) 2000 *Traffic and Granular Flow* (Berlin: Springer)
[7] Prigogine I and Herman R 1971 *Kinetic Theory of Vehicular Traffic* (Amsterdam: Elsevier)
[8] Biham O, Middleton A and Levine D 1992 *Phys. Rev.* A **46** R6124
[9] Nagel K and Schreckenberg M 1992 *J. Phys. I France* **2** 2221
[10] Chung K H, Hui P M and Gu G Q 1995 *Phys. Rev.* E **51** 772
[11] Tadki S I and Kikuchi M 1995 *J. Phys. Soc. Japan* **64** 4504
[12] Cuesta J A, Martines F C, Molera J M and Sanchez A 1993 *Phys. Rev.* E **48** R4175
[13] Nagatani T 1994 *J. Phys. Soc. Japan* **63** 1228
[14] Török J and Kertesz J 1996 *Physica* A **231** 515
[15] Horiguchi T and Sakakibara T 1998 *Physica* A **252** 388
Horiguchi T and Sakakibara T 1998 *Interdisc. Inf. Sci.* **4** 39
[16] Freund J and Pöschel T 1995 *Physica* A **219** 95
[17] Chopard B, Luthi P O and Queloz P A 1996 *J. Phys. A: Math. Gen.* **29** 2325
[18] Chowdhury D and Schadschneider A 1999 *Phys. Rev.* E **59** R 1311
[19] Brockfeld E, Barlovic R, Schadschneider A and Schreckenberg M 2001 *Preprint* cond-mat/0107056
[20] May A D (ed) 1990 *Traffic Flow Fundamentals* (Englewood Cliffs, NJ: Prentice Hall)
Daganzo C F (ed) 1993 *Transportation and Traffic Theory* (Amsterdam: Elsevier)
[21] Robertson D I and Bretherton R D 1991 Optimizing networks of traffic signals in real-time: the SCOOT method *IEEE Transp. Veh. Technol.* **40** 11
[22] Knospe W, Santen L, Schadschneider A and Schreckenberg M 2000 *J. Phys. A: Math. Gen.* **33** L477
[23] Kotz S and Johonson N L 1982 *Encyclopedia of Statistical Sciences* vol 3 (New York: Wiley) p 292
[24] Fouladvand M E and Nematollahi M 2001 *Eur. Phys. J.* B **22** 395
[25] Porche I, Sampath M, Chen Y-L, Sengupta R and Lafortune S 1996 A decentralized scheme for real-time optimization of traffic signal *Proc. 1996 IEEE Int. Conf. on Control Applications* pp 582–9
[26] Faieta B and Huberman B A 1994 *Firefly: A Synchronisation Strategy for Urban Traffic Control* Xerox Palo alto Research Centre, Palo Alto, CA 94304
[27] Lowrie P 1992 *SCATS: A Traffic Responsive Method for Controlling Urban Traffic* Technical report Road and Traffic Authority (Australia: NSW)
[28] Sims A G 1979 SCATS: the Sydney co-ordinated adaptive system *Proc. Eng. Foundation Conf. on Research Priorities in Computer Control of Urban Traffic Systems* p 12